
STRUCTURE, PHASE TRANSFORMATIONS,
AND DIFFUSION

Dynamic Theory of the Effect of a Strong Magnetic Field on the Martensitic Transformation in Steels with Austenite Grain Sizes Close to a Critical Value

M. P. Kashchenko^{a, b, *}, N. M. Kashchenko^a, and V. G. Chashchina^{a, b}

^aUral Federal University, Ekaterinburg, 620002 Russia

^bUral State Forestry University, Ekaterinburg, 620100 Russia

*e-mail: mpk46@mail.ru

Received August 12, 2020; revised September 1, 2020; accepted September 3, 2020

Abstract—In the dynamic theory of martensitic transformations, temperature M_s of the start of transformation corresponds to conditions that are optimal for generating waves by nonequilibrium d electrons that control the growth of a martensitic crystal. The recognition of relative damping Γ'_e of s electrons plays a substantial role in this case. A general analysis that has made it possible to propose, for the first time, an analytical formula for critical size $D_c(\Gamma'_e)$ of austenite grains is used to interpret the results for chromium–nickel steels, in which the transformation is initiated by strong magnetic fields. Under conditions of positive bulk magnetostriction, a magnetic field with intensity H lowers the chemical potential of electrons. As a result, the $D_c(\Gamma'_e, H)$ value decreases and austenite with a grain diameter of D , which was stabilized by condition $D < D_c(\Gamma'_e, 0)$ in the absence of a field, becomes destabilized, since inequality $D > D_c(\Gamma'_e, H)$ is fulfilled. The dynamic theory predicts a sharp increase in the $D_c(\Gamma'_e, 0)$ value at $\Gamma'_e \rightarrow 1$. This is evidenced by value $D_c(\Gamma'_e) \geq 1$ mm for steel 67Kh2N22, which is three orders of magnitude larger than $D_c(\Gamma'_e, 0) \approx 1$ μm for the Fe–31Ni alloy. Other peculiarities of the effect of magnetic field on the martensitic transformation are also discussed.

Keywords: martensitic transformations, dynamic theory, critical grain size, bulk magnetostriction, destabilization of austenite by magnetic field

DOI: 10.1134/S0031918X21010051

INTRODUCTION

Martensitic transformation (MT) in iron alloys occurs with pronounced signs of a first-order phase transition. The growth rate of crystals exceeds the speed of longitudinal elastic waves, which provides unambiguous evidence for the existence and decisive role of the controlling wave process (CWP) that ensures the cooperative nature of the transformation. The start of crystal growth upon cooling to temperature M_s is associated with the appearance of an initial excited (vibrational) state (IVS) in the elastic field of dislocation sites of nucleation (DNSes). Moreover, the CWP inherits information about the strain field in the IVS region and transfers threshold deformation, thereby violating the stability of austenite. The process takes place with a substantial deviation from an equilibrium temperature T_0 of the initial (austenite, γ) and final (martensite, α) phases, i.e., under substantially nonequilibrium conditions.

The above points reflect, in a concise form, the foundations of the new paradigm of the MT embodied in the dynamic theory of MTs [1–5]. The completeness of the description of the γ – α martensitic transformation in the dynamic theory is achieved in view of the fact that the CWP makes it possible to trace the fundamental relationship between the electronic structure features of the γ phase and the elastic fields of DNSes on the one hand and the observed macroscopic morphological features (the so-called “metallurgical visiting card” of the MT) on the other hand. This proves the physical validity and reliability of the dynamic theory.

The derivation of an analytical formula for critical size $D_c(\Gamma'_e)$ of an austenite grain as a function of the relative effective damping of s electrons is among the most important results of the theory.

In this case, the fact that the IVS region has an elongated parallelepiped shape is taken into account

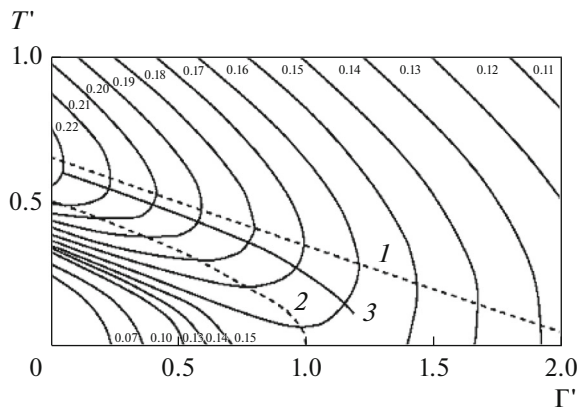


Fig. 1. Results calculating the $\partial f/\partial\mu'$ values [1–3].

and the following characteristic ratio of spatial scales is fulfilled:

$$L/d_m \sim 10^2, \quad (1)$$

where d_m is the transverse size of the IVS region, and L is the size of the grain volume that is free of dislocations (for a single dislocation in the grain, L coincides with grain size D). The m index in notation d_m reflects the choice of the largest transverse size of the IVS region by the system, which is still compatible with the threshold strain conditions of metastable austenite.

When interpreting temperature M_s as an optimal temperature for generation of waves that control the growth of a martensite crystal by nonequilibrium electrons, it is shown that $M_s(\Gamma'_e) \rightarrow 0$ K and, formally, $D_c \rightarrow \infty$ when $\Gamma'_e \rightarrow 1$. Indeed, we can talk in reality about some finite value $(D_c)_{\max} \equiv D^*$ at $\Gamma'^* \leq 1$. Hence, the formation of the martensite of cooling turns out to be impossible for polycrystalline austenite with grain size D if

$$D < D^*, \quad (2)$$

i.e., inequality (2) is the condition for the stabilization of austenite. However, the influence of a strong magnetic field with strength H lowers, especially in the presence of a positive change in the volume due to magnetostriction, chemical potential μ of electrons, which leads to decreases in the Γ'_e and $D_c(\Gamma'_e, H)$ values, so that inequality $D > D_c(\Gamma'_e, H)$ is fulfilled and austenite becomes destabilized. This issue is covered in general form in [3] in relation to the Fe–(30–32%)Ni and Fe–31Ni–0.28C alloys. It is essential that the addition of 0.28 wt % C increases the $D_c(\Gamma'_e)$ value by an order of magnitude (up to 10 μm) in comparison with that for the Fe–31Ni alloy. An explanation for the high growth rate of the Γ'_e value with the addition of carbon is given in [1]; therefore, it is clear that an increase in the carbon content should be

accompanied by a rapid increase in the $D_c(\Gamma'_e)$ value. In this regard, the processing of the published data [6] for the $C_x\text{Kh}2\text{N}22$ steels at carbon concentrations of $x = 0.24, 0.36, 0.45, 0.57, 0.67,$ and 0.77 wt % on the basis of the dynamic theory is of interest. It is the analysis of these data supplemented by the results published in [7] that is the main goal of this study.

FORMULAS FOR M_s AND $D_c(\Gamma'_e)$

We assume that the nonequilibrium state of the electronic subsystem in the interface region at the stage of crystal growth is mainly caused by chemical potential gradient $\nabla\mu$. Hence, the analysis of the values of the derivatives of modified equilibrium Fermi distribution f with respect to chemical potential μ is a basis for choosing the optimal conditions for wave generation. This distribution takes into account the blurring not only due to the temperature factor (directly taken into account in f), but also due to the scattering of s electrons, which is characterized by attenuation of Γ'_s . It should be noted that it is the high attenuation of Γ'_s that provides an acceptable population of d states above (and below) the μ level in the actual energy range due to the $d-s-d$ redistribution processes. Along with $\nabla\mu$, the $\partial f/\partial\mu'$ derivatives specify nonequilibrium corrections to the distribution function, which determine the degree of population inversion for pairs of states of $3d$ electrons that are active in wave generation [1–3]. The idea is to find the optimal trajectories on the plane of dimensionless variables T' and Γ' by formulas

$$T' = \frac{k_B T}{|\bar{\epsilon}_d - \mu|}, \quad \Gamma' = \frac{\hbar \Gamma}{2|\bar{\epsilon}_d - \mu|}, \quad (3)$$

along which the value of the nonequilibrium correction will change relatively slowly with a simultaneous decrease in the T' value and an increase in the Γ' value. Such behavior reflects a situation typical of a decrease in temperature M_s with an increase in the concentration of alloy components additional to iron. In Eq. (3), the $\bar{\epsilon}_d$ value plays the role of the average energy over the energy range $|\bar{\epsilon}_d - \mu| \approx 0.2-0.3$ eV relevant for wave generation, k_B is the Boltzmann constant, and \hbar is the Planck constant. Figure 1 shows the calculation results for $\partial f/\partial\mu'$.

Families of thin lines are constant level lines, at which the $\partial f/\partial\mu'$ function takes constant values (marked on the lines), and dashed lines 1 and 2 are determined, respectively, by conditions

$$\frac{\partial f}{\partial T'} \left[\frac{\partial f}{\partial \mu'} \right]_{\Gamma'} = 0, \quad \frac{\partial f}{\partial \Gamma'} \left[\frac{\partial f}{\partial \mu'} \right]_{T'} = 0.$$

These lines correspond to the maxima of the $\partial f/\partial\mu'$ function with respect to variables T' and Γ' and

pass through the points, at which straight lines that are parallel, respectively, to the vertical and horizontal coordinate axes touch the constant level lines. Solid line 3 in Fig. 1 is a projection of the ridge on the $\partial f/\partial \mu'$ function relief onto the (Γ', T') plane. The region between lines 1 and 2 corresponds to the range of values of the T' and Γ' parameters, for which the inverse population difference reaches the maximum values that weakly vary with a change in the T' and Γ' values.

A rather detailed discussion published in [1] showed that the mapping of the observed $M_s(T)$ dependences for Fe-Ni alloys onto the (Γ', T') plane tends to line 2 described by the following parabola:

$$1 - \Gamma' = 4T'^2. \quad (4)$$

The range between a pair of points $(\Gamma' = 1, T' = 0)$ and $(\Gamma' = 0.96, T' = 0.1)$ that lie on curve (4), which is the most interesting interval for the aims of our study, was additionally processed in [3, 5] by approximations of the following type:

$$1 - \Gamma' = B(T')^P, \quad (5)$$

for $P > 2$.

Here, we use the following simplest approximation of the trajectory between the specified pair of points in the form of a straight line ($P = 1, B = 0.4$):

$$1 - \Gamma' = 0.4T'. \quad (6)$$

The attenuation Γ has several contributions in the following form:

$$\Gamma(T, C, D) = \Gamma(T) + \Gamma_i + \Gamma(D). \quad (7)$$

In Eq. (7), the $\Gamma(T)$ contribution is associated with scattering by thermally activated inhomogeneities (vacancies, phonons, magnons, etc.) and decreases with a decrease in the T value, and the Γ_i contribution is associated with impurity scattering. In the case of a binary alloy, $\Gamma_i = \Gamma(C) \sim C(1 - C)$, where C is the concentration of the alloying addition. The $\Gamma(D)$ contribution is actually due to the influence of an inhomogeneity with characteristic transverse spatial size d_m on the attenuation of s electrons. This inhomogeneity is associated with the release of energy in the IVS region. Taking into account ratio (1) for spatial scales, the scattering by such an inhomogeneity at $L = D$ can be interpreted as a dependence on D . The characteristic time required for s electrons to cross region d_m with velocity v_s is $\tau_s \approx d_m/v_s$; therefore, in accordance with the uncertainty relation for energy and time, the magnitude of scattering is

$$\hbar\Gamma(d) \approx \hbar/2\tau_s \approx \hbar v_s/2d_m. \quad (8)$$

However, it should be noted that there is one more spatial scale associated with transverse size d_{tw} of transformation twins. In turn, the d_{tw} value can be two to three orders of magnitude less than d_m and, consequently, by four to five orders of magnitude less than L

and D . Since grain size D is a convenient parameter for observation, one can use the following explicit expression for $\hbar\Gamma(d)$:

$$\hbar\Gamma(D) \approx \hbar v_s \Phi(L/d)/2D, \quad (9)$$

where $\Phi(L/d)$ is a phenomenological constant that reflects the ratio of scales. It is convenient to choose $\Phi(L/d)$ in the following form:

$$\Phi(L/d) = \beta \times 10^\eta, \quad 1 \leq \beta \leq 10, \quad 2 \leq \eta \leq 5. \quad (10)$$

Hence, according to Eqs. (3), (9), and (10),

$$\Gamma'(D) = \hbar v_s \beta \times 10^\eta / (4|\bar{\epsilon}_d - \mu|D). \quad (11)$$

Further, we assume in the estimates that $v_s = 10^6$ m/s, $\hbar = 1.054 \times 10^{-34}$ J s, and $k_B = 1.38 \times 10^{-23}$ J/K.

The $\Gamma(T)$ contribution, which generally contains several terms with different degrees of temperature dependences, can be expressed as

$$\Gamma(T) = a_0(T)T, \quad (12)$$

or, according to Eq. (3), as

$$\Gamma'(T) = a_0(T)T'/2, \quad (13)$$

where the specific $a_0(T)$ values will be found from additional considerations. We only note that $a_0(T) \approx 1$ at temperatures T differing from 273 by ΔT of around ± 10 K, as an analysis shows [3].

Identifying T with M'_s and substituting expressions for the attenuation of electrons into Eq. (6), we find

$$M_s(D) = M_{s\infty} \{1 - (D_c/D)\}, \quad (14)$$

$$M_{s\infty} = |\bar{\epsilon}_d - \mu| \left(1 - \Gamma'_e\right) / (0.4 + 0.5a_0)k_B, \quad (15)$$

$$D_c = \hbar 10^2 v_s / \left(4|\bar{\epsilon}_d - \mu| \left(1 - \Gamma'_e\right)\right). \quad (16)$$

It should be noted that effective attenuation Γ'_e also includes an additional summand to Γ_i , which takes into account the scattering by short-wavelength vibrations associated with the formation of twins typical of lamellar crystals. We assume that μ depends on H because of the magnetostrictive change of the volume. Using the relationship between μ and concentration n of s electrons ($\mu \sim n^{2/3}$), we obtain

$$\Delta\mu/\mu = -(2/3)\Delta V/V. \quad (17)$$

For $\mu \approx 10$ eV and $\Delta V/V = 10^{-3}$, we find from Eq. (17) that $\Delta\mu \approx -6.7 \times 10^{-3}$ eV, which corresponds to a decrease in the μ value by $\Delta\mu/k_B \approx 77.5$ K on the temperature scale and, consequently, to an increase in parameter $|\bar{\epsilon}_d - \mu|$. It is quite possible to achieve values at a level of $\Delta V/V = 10^{-3}$ in strong fields. For example, $\lambda_H \approx 4.3 \times 10^{-5}$ (MA/m) $^{-1}$ in linear extrapolation

$$\Delta V/V = \lambda_H H \quad (18)$$

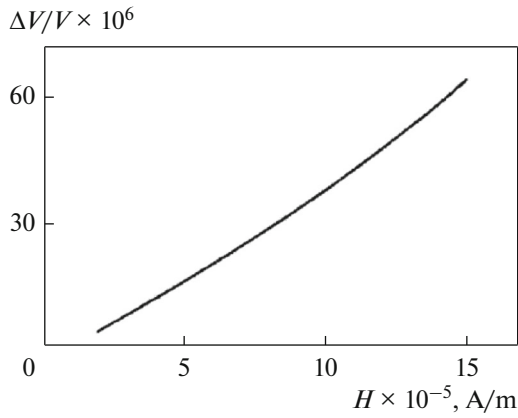


Fig. 2. Change in the volume of the 40Kh2N20 austenite steel in magnetic fields of up to 1.51 MA/m at a temperature of 77 K [8].

as follows from Fig. 2. Hence, we obtain $\Delta V/V \approx 1.55 \times 10^{-3}$ for $H = 36$ MA/m.

For the convenience of comparison with data in the absence of a field, we express the $|\bar{\epsilon}_d - \mu|$ parameter in the following form:

$$|\bar{\epsilon}_d - \mu| = |\bar{\epsilon}_d - \mu_0|(1 + \Delta_H), \quad \mu_0 \equiv \mu_{H=0}, \quad (19)$$

$$\Delta_H = 2\mu_0\lambda_H H / (3|\bar{\epsilon}_d - \mu_0|). \quad (20)$$

Hence, formulas (14)–(16) transform to

$$M(D)_s = M_{s0\infty} \left[1 - \frac{D_{c0}}{D} + \frac{\Delta_H}{1 - \Gamma'_{e0}} \right], \quad (21)$$

$$M_{s0\infty} = |\bar{\epsilon}_d - \mu_0| \left(1 - \Gamma'_{e0} \right) / (0.4 + 0.5a_0)k_B, \quad (22)$$

$$D_c = D_{c0} \left[1 + \Delta_H / (1 - \Gamma'_{e0}) \right]^{-1}, \quad (23)$$

$$D_{c0} = \hbar\beta \times 10^n v_s / \left(4|\bar{\epsilon}_d - \mu_0|(1 - \Gamma'_{e0}) \right).$$

Table 1. Data from [6] and a_0 parameter values

Name of steel brand	M_s , K	$\Delta H/\Delta T$, MA/mK	a_0
24Kh2N22	263	0.256	1
36Kh2N22	177	0.224	0.78220
45Kh2N22	130	0.196	0.63443
57Kh2N22	77	0.182	0.56054
67Kh2N22	4.2	0.161	0.44971
77Kh2N22	–	0.144	0.35999

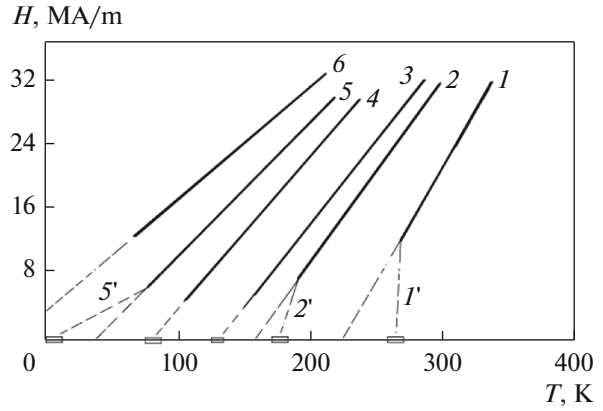


Fig. 3. Dependences $H(T)$ of pulsed magnetic field that initiates a martensitic transformation in steels of the following brands: (1) 24Kh2N22, (2) 36Kh2N22, (3) 45Kh2N22, (4) 57Kh2N22, (5) 67Kh2N22, and (6) 77Kh2N22.

PROCESSING OF THE EXPERIMENTAL DATA

The data from [6] are shown in Fig. 3 and Table 1. The values of temperatures M_s at $H = 0$ correspond to rectangles on the T axis in Fig. 3, and the $\Delta H/\Delta T$ values are the slopes of the linear sections of the $H(T)$ dependences. In addition to the experimental data, Table 1 shows the a_0 values obtained from the correlation between the observed slopes and those found using Eqs. (21) and (20).

To carry out the initial calibration of the $|\bar{\epsilon}_d - \mu|$ and a_0 parameters, which is necessary for data processing, we have to compare the data for one of the steels under consideration with a specific point on line (6). The experience of data processing [3, 5] for Fe–Ni alloys shows that temperature M_s of steel 24Kh2N22 as a trial choice can be compared with point ($\Gamma' = 0.96$, $T = 0.1$). The proximity of M_s to 273 K allows us to consider $a_0 = 1$, while requirement $M'_s = 0.1$ implies $|\bar{\epsilon}_d - \mu| \approx 362.94 \times 10^{-23} \text{ J} \approx 0.22684 \text{ eV}$ or 2630 K on the temperature scale. Let us estimate what slope the selected calibration will lead to. Using Eqs. (21) and (20), we obtain

$$\frac{dH}{dM_s} = 3(0.4 + 0.5a_0)k_B / 2\mu_0\lambda_H. \quad (24)$$

We find $dH/dM_s \approx 0.271$ MA/mK from Eq. (24) for $a_0 = 1$, $\mu_0 \approx 10 \text{ eV} \approx 1.6 \times 10^{-18} \text{ J}$, $\lambda_H \approx 4.3 \times 10^{-5} (\text{MA/m})^{-1}$, and $k_B = 1.38 \times 10^{-23} \text{ J/K}$, which agrees well with the experimental result of 0.256 MA/mK in Table 1. The experimental data can be used to refine λ_H , assuming $\lambda_H \approx 4.552 \times 10^{-5} (\text{MA/m})^{-1}$. Fixing λ_H and μ_0 , we find the a_0 parameter for the remaining alloys by substituting the dH/dM_s value in Eq. (24) with the values given in Table 1. The slow

change in the a_0 parameter is likely to be explained by the significant contribution of the scattering by magnetic inhomogeneities to $\Gamma(T)$ under conditions of a paraprocess in austenite, which has a complex noncollinear magnetic structure.

It should be noted that there are nonlinear sections in the region of weak fields, along with the linear dependence $H(M_s)$ in strong fields. Conditionally, these sections in Fig. 3 are replaced by linear segments 1', 2', and 5'. Segments 1' and 2' with large slopes reflect the presence of a superparamagnetic state of austenite. Indeed, the presence of misaligned ferromagnetic clusters upon application of a weak field is accompanied by the appearance of magnetization largely due to the reversal of the magnetic moments and displacement of domain walls upon an insignificant change in the volume, which corresponds to small values of the λ_H parameter in Eq. (24) and, consequently, to a large dH/dM_s value. Another peculiarity (conditionally reflected by line 5') is caused by an increase in the λ_H and will be discussed below.

It should be noted that austenite with grain sizes in the range of $D = 5\text{--}7$ mm was used in [6] to prepare samples, from which single crystal cylinders with a diameter of 3–5-mm and a generatrix length of 12 mm were made for measurements. Therefore, we take $D = 5$ mm for definiteness. After this choice, which is somewhat conditional but sufficient for estimating the orders of magnitude, one can use Eqs. (20)–(22) to find D_{c0} and D_c . It is clear in advance that the proximity of M_s to 0 K for an alloy with 0.67 wt % carbon means the existence of a certain carbon concentration in the range of $C_D > 0.67$ wt %, at which equality $D_{c0} = D$ is satisfied. It is also obvious that inequality $D_{c0} > D$ is fulfilled for steel 77Kh2N22. The data processing was performed for parameters $\beta = 1$ and $\eta = 2$, and for $\beta = 4$ and $\eta = 3$. Table 2 shows the rounded results of calculations for ($\beta = 4$, $\eta = 3$) and fixed values $|\epsilon_d - \mu_0| = 0.22684$ eV, $D = 5$ mm, $\Gamma'(D) = 5.78608 \times 10^{-3}$, $\lambda_H = 4.552 \times 10^{-5}$ (MA/m) $^{-1}$, $H = 32$ MA/m, and $\Delta_H = 0.042096$.

Let us comment on the data given in Table 2.

(1) Added concentration $C_D \approx 0.69343$ wt % C (at $D_{c0} = D$ and $M_{s0} = 0$) was estimated based on the linear interpolation of the concentration rate of changing D_{c0}/D upon the transition from 0.57 to 0.67 wt % C.

(2) The case with 0.77 wt % C formally corresponds to $M_{s0} = -22.2$ K and $D_{c0} > D$.

(3) According to Eq. (21), the temperature shift M_s can be calculated by the following expression:

$$\Delta M_s = M_{s0\infty} \left[\frac{\Delta_H}{1 - \Gamma'_{c0}} \right]. \quad (25)$$

Table 2. Results of processing the published data [6]

Carbon content, wt %	$M_{s0\infty}$, K	ΔM_s , K	$\frac{D_{c0}}{D}$	$\frac{D_{cH}}{D_{c0}}$	Γ'_e
0.24	280	123	0.060	0.695	0.9042
0.36	196	140	0.098	0.584	0.9410
0.45	151	154	0.163	0.495	0.9588
0.57	99.4	162	0.225	0.379	0.9743
0.67	28.6	177	0.853	0.139	0.9932
C_D	24.7	179	1	0.121	0.9942
0.77	4.0	190	6.530	0.020	0.9991

RESULTS AND DISCUSSION

(1) The data published in [6] support the conclusion drawn from the dynamic theory that critical grain size D_{c0} increases with an increase in the relative attenuation of s electrons ($\Gamma'_e \rightarrow 1$). Actually, an increase in the carbon content from 0.24 to 0.77 wt % is accompanied by an increase in the D_{c0} value by two orders of magnitude with reaching the region of $D_{c0} \approx 1$ cm.

Recall that most studies (see, for example, [9–14]) contain a qualitative statement about the existence of a critical grain size, while typical quantitative estimates of D_{c0} were around 1 μm (10 μm in [11] and 25.4 μm in [14]).

(2) The desire to clarify the $H(M_s)$ dependence in the region of low temperatures and fields [7] led to interesting results that are reflected in Fig. 4.

The comparison of Fig. 3 with Fig. 4 shows, first, that there is no martensite of cooling in the case of steel 67Kh2N22 [7]. In the light of the performed calculations, this is easily explained by the fact that

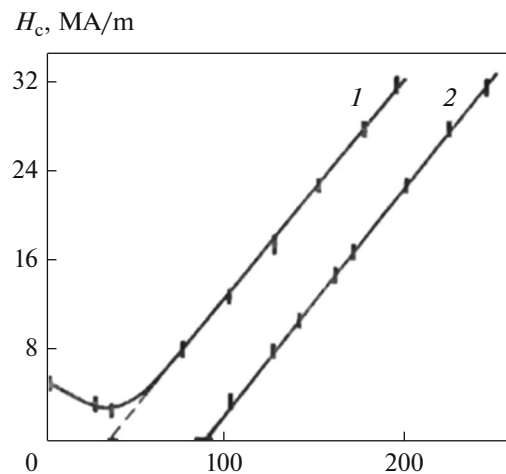


Fig. 4. Temperature dependences of the critical magnetic field of chromium–nickel steels (1) 67Kh2N22 and (2) 50Kh2N20 [7].

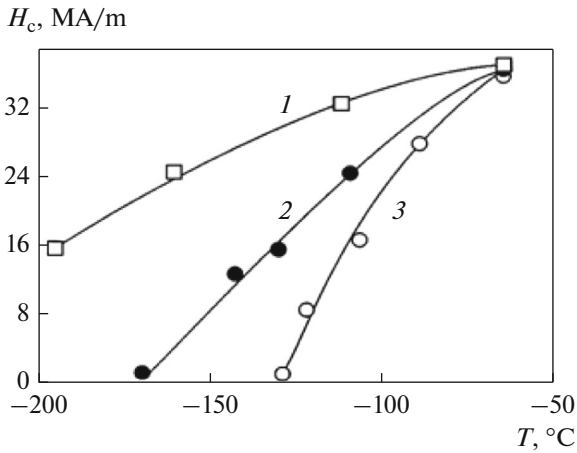


Fig. 5. Temperature dependences of the threshold magnetic field for the Fe–31% Ni–0.25C alloy with grain sizes D [17, 18] of (1) 16, (2) 45, and (3) 180 μm .

inequality $D_{c0} > D$ is satisfied for the samples from [7]. In actual fact, it follows from Table 2 that $D_{c0} \approx 0.853$ mm and $D \approx 4.26$ mm. The diameters of the cylindrical samples in [7] are smaller (1.2 and 3 mm, respectively) than those published in [6] and less than the estimated D_{c0} value. In addition, homogenizing annealing (for 6 h in [7] and for 12 h in [6]) should lead to the formation of crystals with a subgrain structure at scales of $L < D_{c0}$, along with the crystals whose bulk is free of DNSes. In our opinion (see [15]), the existence of subgrain boundaries is confirmed by the observed packets of parallel martensite crystals that are not only synchronously excited at grain boundaries, but also kinked at such boundaries. Secondly, a minimum at $T \approx 38$ K is reliably identified on the $H(M_s)$ dependence, which clearly indicates changes in the magnetic structure of austenite that has, according to [7], a maximum of initial magnetic susceptibility $\chi_0(T)$ at $T \approx 28$ K. In [7], this feature of $\chi_0(T)$ is presumably associated with magnetic ordering in an essential part of austenite, which was delayed (because of the mixed nature of the exchange interaction) with respect to the ferromagnetic transformation at 70 K and led to the formation of ferromagnetic clusters. Assuming that the transition from weak magnetic fields (at which $\chi_0(T)$ was observed) to critical fields is accompanied [16] by an increase in temperature θ corresponding to the maximum of χ , it is natural to relate the minimum on the $H(M_s)$ curve to the maximum of λ_H . This can be easily reflected in formula (24) by specifying λ_H , as follows:

$$\lambda_H = \lambda^* - b(T - \theta)^2, \quad b = \text{const} > 0, \quad (26)$$

where λ^* is the maximum value of λ_H at $\theta = 38$ K, which corresponds to $H_{\min} \approx 2.9$ MA/m (Fig. 4). The beginning of line 1 at $T = 0$ corresponds to $H \approx 5.3$ MA/m. For the linear section of line 1, $dH/dT \approx 0.195$ exceeds value 0.161 we used earlier (see Table 1).

Taking into account the qualitative nature of the estimates, we refer this change to a_0 , assuming $a_0 \approx 0.63$ and retaining the previously used values of $\lambda_H = 4.552 \times 10^{-5} (\text{MA/m})^{-1}$ for the linear section. To determine the values of three unknown parameters (D_{c0}/D , b , and λ^*), we write expression (22) for three points, taking into account Eq. (26) and adding the third point of the graph to the right of the minimum, i.e., $T_3 \approx 61.5$ K and $H_3 \approx 5.3$ MA/m, to the two ones indicated above ($T_1 = \theta = 38$ K and $H_1 = H_{\min} \approx 2.9$ MA/m; and $T_2 = 0$ and $H_2 \approx 5.3$ MA/m). Solving the system of three equations, we obtain that $D_{c0}/D \approx 1.28$, $b \approx 1.05 \times 10^{-7} \text{K}^{-2}(\text{MA/m})^{-1}$, and $\lambda^* \approx 12.84 \times 10^{-5} (\text{MA/m})^{-1}$. It is easy to check using Eq. (26) that the λ_H value for the linear section of the $H(T)$ dependence is achieved at $T_4 \approx 66.1$ K, so that λ_H should be assumed to be constant at $T \geq T_4$ and almost three times less than λ^* . Thus, a decrease in the slope (a twofold decrease with a rough linear description) of section 5' in Fig. 3 has an understandable origin. The expression for λ_H can be easily modified to describe sections 1' and 2' that reflect its decrease in Fig. 3.

(3) It follows from the results of analyzing the data given in Table 2 that shift ΔM_s increases with a decrease in temperature M_s . This is caused by a decrease in the D_c value in the presence of a magnetic field. A decrease in the D_c value is accompanied by the well-known effect of destabilization of austenite [17], which can be stabilized either by grain refinement or plastic deformation, so that condition $D < D_{c0}$ (or $L < D_{c0}$) is satisfied. In a strong field, $D > D_{cH}$ and the region with $M_{sH} > 0$ K exists.

(4) At a fixed chemical composition of the alloy, temperatures M_{soi} of the spontaneous MT are different for different grain sizes D_i . However, if $D_{cH} \ll D_i$ in a strong field, then the D_c/D value can be neglected and, according to Eq. (14), $M_{sH} = M_{sH\infty}$, i.e., all $H(M_{sH})$ curves tend to one point, which is observed (Fig. 5).

(5) When turning to parameters $\beta = 1$ and $\eta = 2$ and keeping $D = 5$ mm, the D_{cH}/D_{c0} values change insignificantly, while the D_{c0}/D values, as well as shifts ΔM_s , decrease substantially.

(6) As noted above, attenuation $\Gamma(D)$ physically corresponds to $\Gamma(d_m)$; therefore, the d_{mc}/d_m ratio stands behind the D_c/D ratio and

$$d_{mc} = \hbar v_s / \left(4 |\bar{\epsilon}_d - \mu| \left(1 - \Gamma'_c \right) \right). \quad (27)$$

Since the magnetic field leading to an increase in the specific volume should lead to a decrease in the interfacial energy/strain threshold, the region of localization of IVSes in the elastic field of DNSes will move away from the DNSes, which will lead to an increase in the d_m value. This should be accompanied by an increase in the thickness of the resulting crystals with an increase in the magnetic field strength. This effect was identified in [17] as a transition from thin lamellar

martensite to lamellar martensite. In this regard, it is appropriate to note that the d_{mc}/d_m parameter in a strong field decreases not only because of a decrease in the d_{mc} value, but also owing to an increase in the d_m value.

(7) It is also pertinent to recall that the specific orientational effect of the formation of martensite crystals in a strong magnetic field is predicted by the dynamic theory [19] and experimentally confirmed in [20].

CONCLUSIONS

An analysis of the experimental data published in [6] and [7] shows that the dynamic theory of MTs adequately describes the observed features of MTs in strong magnetic fields.

The morphological analysis, which is systematized in [17] and genetically related to elastic fields of DNSes in the dynamic theory, is a reliable basis for drawing conclusions.

An increase in the specific volume upon MTs plays a substantial role in magnetostriction and determines the specific features of the transformation without changing its physical nature. Therefore, the concept of hypothetical microscopic nuclei of martensite, as well as attempts to interpret MTs in strong magnetic fields as a first-order magnetic phase transition [21], are irrelevant.

FUNDING

The authors acknowledge support from the Ministry of Science and Higher Education of Russia via the state assignment no. 075-00243-20-01 of 08/26/2020 within the framework of the FEUG-2020-0013 theme *Environmental Aspects of Rational Nature Management*.

REFERENCES

1. M. P. Kashchenko, *Wave Model of Martensite Growth at γ - α Transformation in Iron-Based Alloys*, 2nd ed. (Regulyarnaya i Khaoticheskaya Dinamika, Moscow, 2010) [in Russian].
2. M. P. Kashchenko and V. G. Chashchina, "Dynamic model of supersonic martensitic crystal growth," *Phys.-Usp.* **54**, 331–349 (2011).
3. M. P. Kashchenko and V. G. Chashchina, *A Dynamic Model of the Formation of Twin Martensitic Crystals at γ - α Transformations in Iron-Based Alloys* (Regulyarnaya i Khaoticheskaya Dinamika, Moscow, 2010) [in Russian].
4. M. P. Kashchenko and V. G. Chashchina, "Critical grain size in the $\gamma \rightarrow \alpha$ martensite transformation. Thermodynamic analysis with regard to spatial scales characteristic of martensite nucleation," *Phys. Mesomech.* **13**, 189–194 (2010).
5. M. P. Kashchenko and V. G. Chashchina, "Grain size dependence of the $\gamma \rightarrow \alpha$ martensite transformation starting temperature," *Phys. Mesomech.* **13**, 195–202 (2010).
6. A. A. Leont'ev, Candidate's Dissertation in Physics-Mathematics (Sverdlovsk, 1985).
7. L. N. Romashov, A. A. Leont'ev, and V. D. Sadovskii, "Martensitic transformation in chromium-nickel steel in magnetic field at the temperatures below 77 K," *Fiz. Met. Metalloved.* **66**, 935–942 (1988).
8. I. V. Zolotarevskii, S. V. Loskutova, V. L. Snezhnoi, and L. M. Sheiko, "Magnetostriction of the paraprocess of austenitic alloys near the martensite point," *Fiz. Met. Metalloved.* **47**, 1312–1313 (1979).
9. E. Scheil, "Über die Umwandlung des Austenit in geharten Stähle," *Z. Anorg. Chem.* **180**, 1–6 (1929).
10. M. G. Gaidukov and V. D. Sadovskii, "Effect of austenite grain size on martensitic transformation in steel," *Dokl. Akad. Nauk SSSR* **96**, 67–69 (1954).
11. M. Umemoto and W. S. Owen, "Effects of austenitizing temperature and austenite grain size on the formation of athermal martensite in an iron-nickel and an iron-nickel-carbon alloy," *Metall. Trans.* **5**, 2041–2046 (1974).
12. Yu. F. Ivanov, M. P. Kashchenko, A. B. Markov, and V. P. Rotshtein, "The critical grain size for the nucleation of α -martensite," *Zh. Tekh. Fiz.* **65**, 99–102 (1995).
13. E. N. Blinova, A. M. Glezer, N. B. D'yakonova, and V. A. Zhorin, "Size effect during martensitic transformation in iron-nickel alloys quenched from the melt," *Izv. Ross. Akad. Nauk, Ser. Fiz.* **65**, 1444–1449 (2001).
14. M. P. Kashchenko, N. M. Kashchenko, A. V. Korolev, S. A. Oglezneva, and V. G. Chashchina, "Critical grain size estimation in the γ - α martensitic transformation with athermal macrokinetics by the example of Fe-Ni-Cr system," *Phys. Mesomech.* **22**, 203–208 (2019).
15. M. P. Kashchenko and V. G. Chashchina, "Dynamic interpretation of formation of parallel thin-plate martensite crystals in strong magnetic fields," *Met. Sci. Heat Treat.* **56**, 343–346 (2014).
16. K. P. Belov, "Ferromagnets and antiferromagnets near the Curie point," *Usp. Fiz. Nauk* **65**, 207–256 (1958).
17. V. M. Schastlivtsev, Yu. V. Kaletina, and E. A. Fokina, *Martensitic Transformation in Magnetic Field* (Ural Branch, Russian Academy of Sciences, 2007) [in Russian].
18. E. A. Fokina, L. V. Smirnov, V. N. Olesov, V. M. Schastlivtsev, Yu. V. Kaletina, and A. Yu. Kaletin, "Influence of austenite grain size on the features of martensitic transformation during cooling and magnetic treatment of Fe-Ni-C alloys," *Fiz. Met. Metalloved.* **81**, 103–111 (1996).
19. M. P. Kashchenko, "Interpretation of a number of specific morphological features of martensite of the Fe-Ni and Fe-C systems in the phonon maser model," *Fiz. Met. Metalloved.* **58**, 862–869 (1984).
20. A. A. Leont'ev, V. M. Schastlivtsev, and L. N. Romashov, "Habit and orientation of martensite crystals formed in a magnetic field," *Fiz. Met. Metalloved.* **58**, 950–957 (1984).
21. I. V. Zolotarevskii, S. V. Loskutova, and M. O. Shchetinina, "Influence of the magnetic state of austenite on the martensitic transformation in Fe-Ni alloys," *Fiz. Met. Metalloved.* **119**, 794–801 (2018).

Translated by O. Kadkin